IOP Conf. Series: Materials Science and Engineering **516** (2019) 012043 doi:10.1088/1757-899X/516/1/012043

Antenna system of ultrawideband borehole radar based on loaded electric dipoles

E V Balzovsky, Yu I Buyanov, V I Koshelev

Institute of High Current Electronics SB RAS, Tomsk, Russia
E-mail: bev@lhfe.hcei.tsc.ru

Abstract. The design of an ultrawideband borehole radar antenna system based on loaded electric dipoles is presented. The antennas are designed to operate in a dielectric medium in the frequency range of 0.25–1 GHz. The results of calculations and measurements of antenna characteristics are presented. The results of sounding the objects when placing antennas in a medium with a relative permittivity of 4 are presented as well.

1. Introduction

When drilling exploratory boreholes, an important task is to determine the position and dielectric properties of oil-saturated reservoirs or water-filled cavities. It is also necessary to determine the boundaries of fractures and high hardness rocks to prevent contact of drilling tools with them. The use of ultrawideband (UWB) electromagnetic pulses allows measuring the parameters of the medium and determining the presence and position of inhomogeneities near the well. This is achieved due to the high resolution of UWB pulses and possibility of time selection of signals reflected from areas with a high gradient of conductivity and/or permittivity.

There are known designs of UWB borehole radars in which the transmitter and receiver are in the same dielectric body - probe. When sounding the medium for reflection, the probe moves over a predetermined distance [1]. The receiver and the transmitter can also be located in different wells, allowing cross-hole studying the environment [2].

The use of semiconductor pulse generators of nano- and sub-nanosecond duration with an amplitude of several kilovolts is promising for increasing the range of UWB borehole radar sounding. At such voltages, the antennas of the receiver and transmitter should be spaced apart and the input port of the receiver should be protected from a high-power radiation pulse. The dipole antennas have the minimum of the pattern in the axial direction, the choice of coaxial dipoles as antennas of such radar reduces the effect of high-voltage radiation pulse on the input port of the receiver.

In this paper the antenna system of the UWB borehole radar is presented. It has been designed to operate in a medium with a dielectric constant $\varepsilon = 4$ when sounding by short pulses with a frequency spectrum of 0.25–1 GHz. A pulse generator with a half-height duration of 0.8 ns, an amplitude of 2.5 kV, and a repetition rate of up to 10 kHz was used as a pulse source. The used generator is specified to be loaded on 50 Ohms at low frequencies and direct current. This feature of the generator determined the design of the antenna system of borehole radar. The antenna should be matched to the generator from the lowest frequencies. The paper presents a description of the design and the results of modeling and measuring the characteristics of the antenna.

2. Antenna system design

To test the functionality of the receiving and transmitting system, a model of the UWB borehole radar was created. The model includes a pulse generator, two antennas in a common dielectric housing, and a digital stroboscopic oscilloscope. The radar is based on two identical dipole antennas 1 and 2 (Figure 1) located in a dielectric housing 3 with an external diameter of 120 mm, internal diameter of 65 mm, and a length of 3.5 m. The housing is placed in a box 4 filled with a model medium. We used the wet sand with a relative permittivity characteristic of sand-oil and sand-drilling fluid mixtures [3]. The distance D between the centers of dipoles varied to find the optimal value. Both antennas can move along the dielectric body axis with a fixed D to scan and record the reflected pulses from the objects on the top surface of the box.

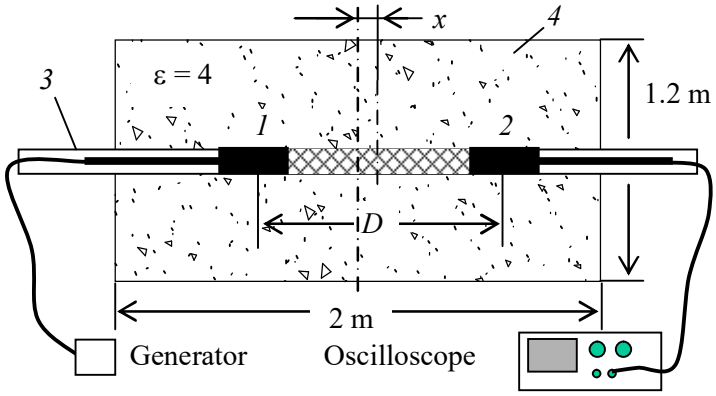

Figure 1. Drawing of experimental setup.

The borehole radar antenna is an electric dipole with an extended bandwidth. The arms of the dipole 1 and 2 (Figure 2) have a cylindrical shape with a cone at central feed point. The length of the dipole is 135 mm. The internal wire of the RG213 coaxial cable is attached to the arm 1 of the dipole, and the cable braid is connected to the arm 2. To reduce the frequency dependence of the input impedance of the dipole, its transverse dimensions are increased due to the metal ribs 3. The entire space between the plates 4 and 5 is filled with a dielectric with $\varepsilon = 3.5$.

To expand the frequency band of antenna matching to the low frequencies, the plates 4 and 5 of the dipole are connected to each other by four metal rods 6 with series-connected resistors 7 and 8 having a nominal value of 100 Ohms. The rods and ribs form segments of strip lines. The choice of the diameter of the rods and the distance to the ribs and cylindrical surface of the dipole arms has improved antenna matching in the frequency range of 0.5–1 GHz.

To reduce the influence of the currents induced on the outer surface of the tube 9 in which the coaxial cable is mounted, the short-circuited segments of coaxial lines (so called “locking cups”) 10 of the length 125 mm and wave impedance of 95 Ohms are used. They are located at a distance of 30 mm from each other and from the plate 4 of the dipole. The external diameter of the antenna is 64.5 mm, and the length is 620 mm including three locking cups. The antennas are placed in a fiberglass tube 11 with a dielectric permittivity $\varepsilon = 4.6$ and a wall thickness of 27 mm.

3. Transceiver parameters

Characteristics of the borehole radar transceiver were measured with a stand which simulates the borehole. The antennas were placed horizontally in a fiberglass tube along the axis of a wooden box filled with moistened sand. Internal dimensions of the box were the following: length 2 m, height and width 1.2 m. The dielectric permittivity $\varepsilon = 3.9$ of the model medium was determined by measuring the delay time of propagation of radiation pulses with a duration of 0.7, 1.5 and 3 ns emitted by UWB combined antenna [5] through the medium and in the free space at the same distance. The frequency dependence of the electromagnetic wave attenuation in the medium was calculated from the ratio of

the spectra of the received pulses that passed through the medium and through free space at a distance of 1.2 m between the receiving and transmitting antennas. The results are shown in Figure 3.

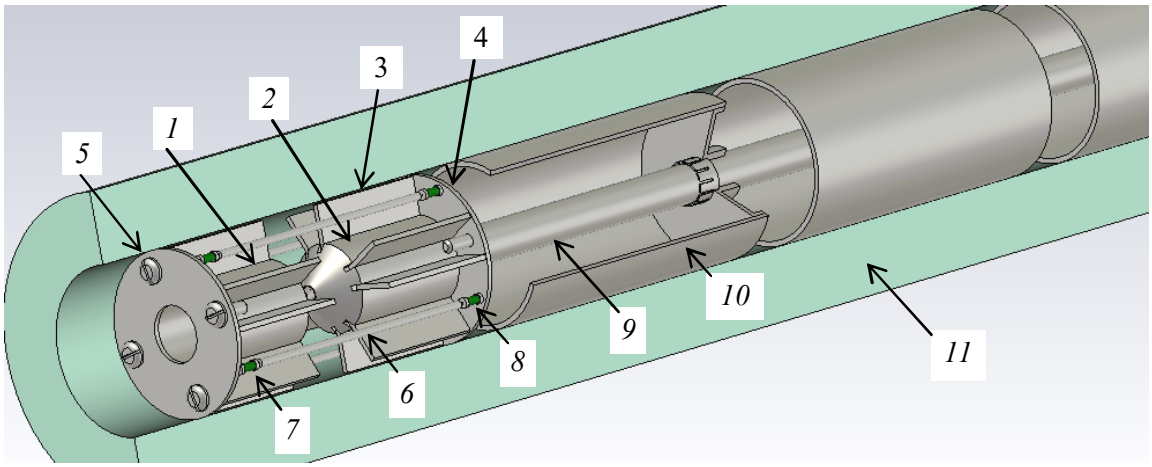

Figure 2. Design of the antenna.

The voltage stand-wave ratio (VSWR) of a single antenna placed in a medium with a 5 m long cable, measured using a vector network analyzer is shown in Figure 4 (curve 1). The VSWR calculated from the ratio of the spectrum of the pulse reflected from the antenna and the spectrum of pulse of the generator is shown in Figure 4 (curve 2). The VSWR of the antenna obtained by the numerical simulation is shown in Figure 4 as well (curve 3).

The pulse waveform at the output of the generator is shown in Figure 5 (curve 1). The waveforms of the generated field strength on the lateral surface of the box are shown in Figure 5. Curve 2 corresponds to measured waveform by using the received UWB dipole [6, 7]. The receiving dipole has the effective height equal to 0.3 cm in the frequency range of 0.2–1.8 GHz. The waveform distortions of the recorded pulses do not exceed 24% compared to the standard TEM antenna. Curve 3 corresponds to calculated waveform.

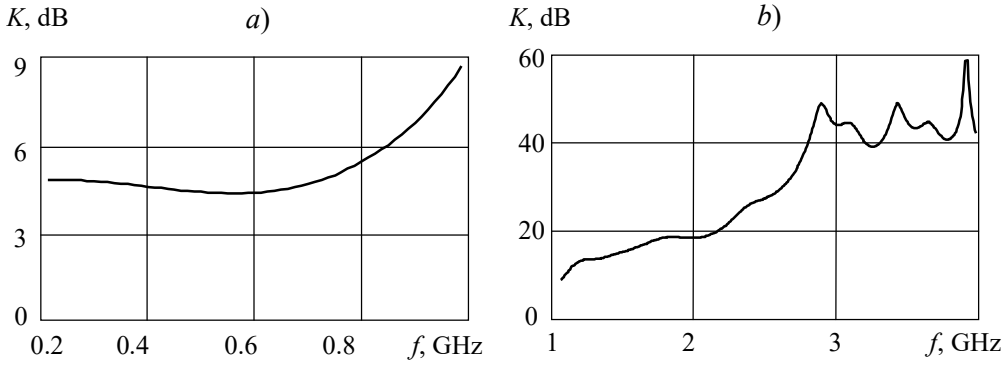

Figure 3. Wave attenuation in the medium at a distance of 1.2 m.

The calculated radiation patterns of the antenna in the medium are shown in Figure 6. The maximum of pattern is perpendicular to the antenna axis in the frequency range of 0.25–0.9 GHz. At higher frequencies, the pattern is distorted. Results of measurement (curve 1) and calculation (curve 2) of the interaction between the transmitting and receiving antennas are shown in Figure 7. We have chosen $M = |U_p^{rec}| / |U_p^{gen}|$ as an estimation of interaction, where U_p^{rec} is the peak value of the voltage at the output of the receiving antenna and U_p^{gen} is the voltage at the input of the transmitting antenna. Figure 7 shows the results of measurement (curve 1) and calculation (curve 2) of the interaction

between the transmitting and receiving antennas. At $D > 60$ cm and $|U_p^{gen}| = 2.5$ kV the peak output voltage of the receiving antenna does not exceed 3 V. The peak electric field strength at a distance of 60 cm from the dipole axis is 450 V/m.

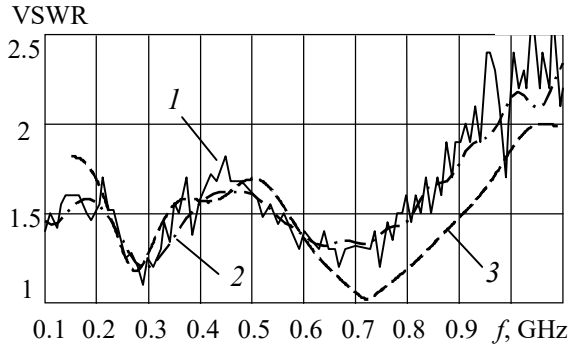

Figure 4. VSWR of the antenna. 1 – measured by network analyzer, 2 – measured in time domain, 3 – simulation.

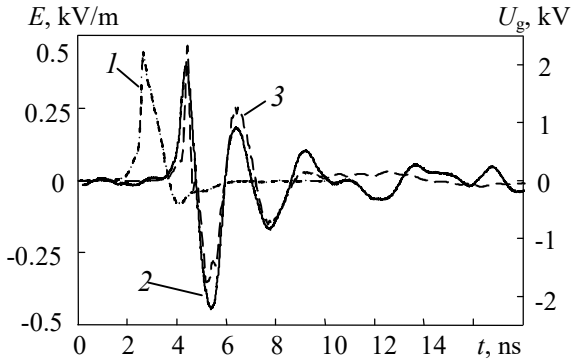

Figure 5. Generator pulse (1); measured (2) and calculated (3) antenna radiation field.

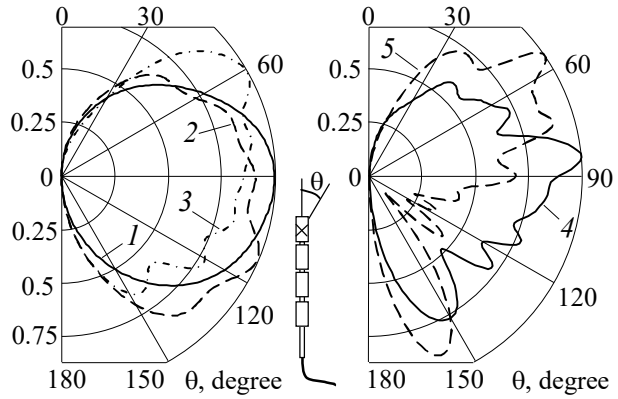

Figure 6. Calculated antenna patterns. 1 – 0.25; 2 – 0.4; 3 – 0.6; 4 – 0.9; 5 – 1 GHz.

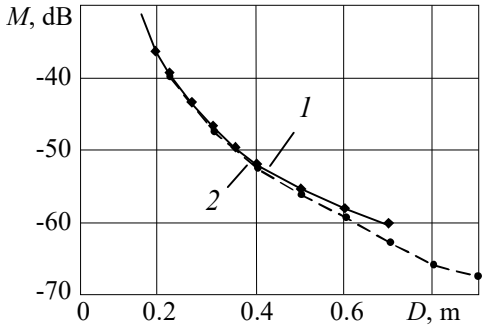

Figure 7. Interaction between transmitting and receiving antennas. 1 – measurements; 2 – simulation.

4. Object sounding results

The sounding was carried out by moving the receiving and transmitting antennas in 5-cm steps inside the fiberglass tube. The tube was placed horizontally in the container with the wet sand. The distance from the axis of antenna displacement to boundaries of the medium was equal to 60 cm. The distance between the antennas $D = 60$ cm was fixed by a polyester-styrene foam rod. The pulse at the output of the receiving antenna was recorded every 5 cm of antennas moving inside the tube. The results were displayed as a set of waveforms $U(t, x)$ in grayscale. Positive voltage corresponds to the light areas and negative one to the dark areas, respectively. The results of sounding of a 140-mm diameter and 400-mm length metal cylinder on the top surface of the box are shown in Figure 8. Area 1 in Figure 8*a* corresponds to the direct radiation from the transmitting antenna, area 2 – to the reflection from the ends of the container with medium which are perpendicular to the axis of scanning, and area 3 – to the reflection from the object, respectively. The result obtained by subtracting the x-averaged voltage $\langle U(t_0, x)\rangle$ from the original waveforms for each fixed time moment t_0 is shown in Figure 8*b*. The difference between waveforms in the presence of an object and waveforms without the object is shown in Figure 8*c*. The time of reflection appearance corresponds to the distance from the object to the axis of scanning. Localization along the x axis corresponds to the length of the object.

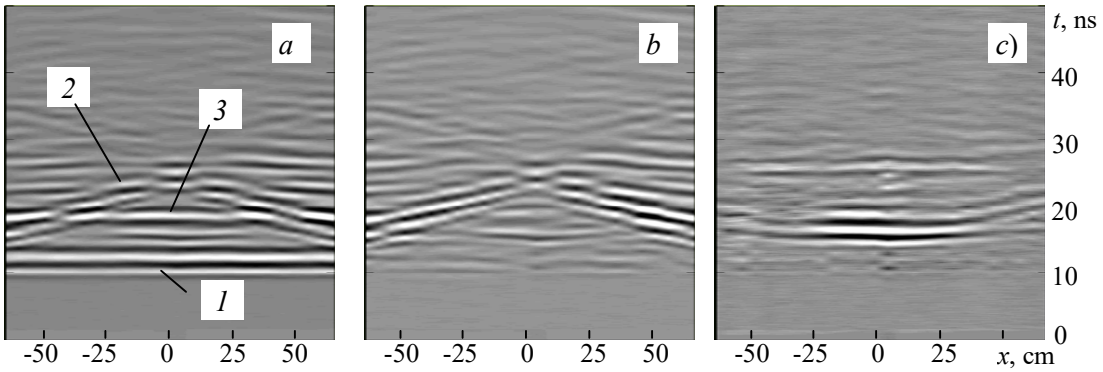

Figure 8. Results of scanning of a metal cylinder on the top surface of box with medium.

Results of scanning of a 105×85 cm metal sheet on the top surface of the container with dielectric medium are shown in Figures 9*a–c*. The sheet was oriented by its narrow side along the axis of scanning. The size and the time of appearance of the reflection area in the Figure 8 correspond to the predetermined place and size of the object. Results of sounding of two 100×35 cm metal plates at a distance of 30 cm from each other are shown in Figures 9*d–f*. Objects are come out at the specified distance to the axis of scanning. The results indicate the possibility to obtain information about the presence of inhomogeneities in the medium with minimal processing of the initial data.

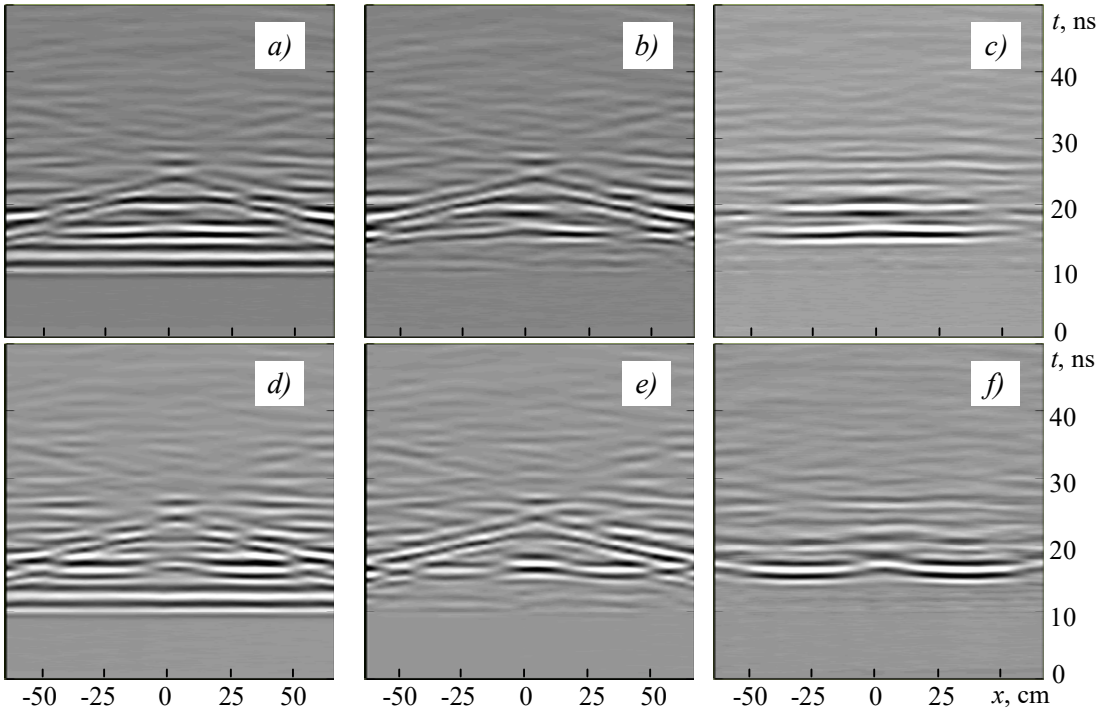

Figure 9. Results of scanning of objects on the top surface of box with medium: the metal sheet (a–c) and two metal plates (d–f).

5. Conclusion

The antenna system of ultrawideband borehole radar based on a dipole with resistive loads has been developed and investigated. The antenna system is intended to sounding the medium nearby the borehole with nanosecond pulses. If the antenna is excited by a monopolar voltage pulse with duration of 0.8 ns at half-height and amplitude of 2.5 kV, the peak electric field strength at a distance of 60 cm from the dipole axis has the value of 450 V/m.

References

[1] Boger M, Glasmachers A 2013 *Proc. 7th Int. Workshop on Advanced Groung-Penetr. Radar* 6601551 doi: 10.1109/IWAGPR.2013.6601551
[2] Zhou H, Sato M 2004 *IEEE Trans. Geosci. Remote Sensing* **42** 335 doi: 10.1109/TGRS.2003.817215
[3] Epov M., Mironov V., Bobrov P., Repin A. 2009 *Rus. Geol. and Geophys.* **50** 470 doi: 10.1016/j.rgg.2009.04.004
[4] Andreev Yu., Buyanov Yu., Koshelev V. 2005 *J. Commun. Technol. Electron* **50** 535
[5] Balzovsky E., Buyanov Y., Koshelev V. 2004 *J. Commun. Technol. Electron* **49** 426